

Combined breakdown in semiconducting bismuth-antimony alloys

E. V. Bogdanov, V. V. Vladimirov, and V. N. Gorshkov

Physics Institute, Ukrainian Academy of Sciences

(Submitted 29 August 1982)

Zh. Eksp. Teor. Fiz. 84, 1468–1473 (April 1983)

The *S*-shaped current-voltage characteristics of $\text{Bi}_{1-x}\text{Sb}_x$ alloys is investigated experimentally and theoretically. It is shown that this shape is due to combined interband breakdown, wherein impact ionization is caused both by the external electric field and by the Hall field, the strength of the latter being determined by the magnetic field of the plasma current. Negative differential resistance appears at currents such that, on the one hand, impact ionization develops intensively, and on the other the pinch effect is not yet fully developed. The phenomenon becomes more intense if the rate of impact ionization is higher in the Hall field than in the applied field.

PACS numbers: 72.20.My, 72.20.Ht, 72.80.Jc

1. The electrophysical and optical properties of $\text{Bi}_{1-x}\text{Sb}_x$ alloys, which are promising for applications in far-infrared devices, have been intensively investigated in the past few years. Owing to the low width of the forbidden band ($\epsilon_g < 23$ meV) and the high carrier mobility ($\mu > 10^6$ cm²/V sec), impact ionization (interband breakdown) takes place in these alloys at external electric field intensities $E \gtrsim 1$ to 10 V/cm and a sufficiently dense plasma ($n \approx 10^{14}$ – 10^{16} cm⁻³) is produced in the sample. All the pinch-effect attributes, wherein the plasma is compressed to the axis of the magnetic self-field of the current, are observed already at currents $I \approx 1$ to 2 A (Ref. 1). In the state preceding the pinch, when the sample is oriented along the binary or bisector axis ($E \parallel C_2, C_1$) a section with negative differential resistance is observed¹ on the current-voltage characteristics (CVC) (*S*-shaped CVC), Fig. 1a. The mechanism of this phenomenon has remained unclear. The purpose of the present paper is therefore to determine the mechanism of the negative differential resistance (NDR) in the alloys in question under impact-breakdown conditions. We have performed additional experiments and developed a theory of *S*-shaped CVC in $\text{Bi}_{1-x}\text{Sb}_x$ alloys. We shall show that this phenomenon is due to combined interband breakdown, wherein impact ionization is due both to the external electric field and to the Hall field (E_H) whose intensity is determined by the magnetic self-field H of the plasma current (transverse breakdown²). Owing to the high carrier mobility, E_H is comparable with E already at $H \approx 10$ –20 Oe and plays a noticeable role in the dynamics of impact breakdown. In the given-field regime (the very one in which the CVC were measured¹) a larger current (larger E_H) can correspond to a smaller value of E . With further increase of the current, the plasma is compressed towards the sample axis (pinch effect), the electron-hole scattering and Auger recombination increase, and the NDR section vanishes. Thus, in accord with the experimental data, NDR is observed in the current region where, on the one hand, impact ionization develops intensively and on the other the pinch effect has not yet evolved sufficiently.¹⁾ The NDR effect is enhanced if the rate of impact ionization in the direction of the Hall field is higher than in the direction of the applied field. This anisotropy of the range g of impact ionization, as shown by our measurements, takes place when

the samples are oriented along the binary and bisector axes ($E \parallel C_2, C_1$). We observed no *S*-shaped CVC for orientation along the trigonal axis ($E \parallel C_3$) (Fig. 1b).

2. We report below results of experiments that have enabled us to determine a number of volume-recombination parameters ($g, \mu_{e,h}$) and characteristics needed to calculate the CVC. The measurements were made by the procedures described in Refs. 1 and 4, at a temperature $T = 4.2$ K.

Samples of *n*-type $\text{Bi}_{0.9}\text{Sb}_{0.1}$ with $n_0 = 10^{14}$ cm⁻³, measuring $0.3 \times 0.3 \times 4$ mm, were cut along the axes C_1, C_2 , and C_3 . The static CVC were determined in the given-current regime (Fig. 1). The inset (Fig. 1a) shows the characteristic time scans of the field intensity E , which make it possible to follow the evolution of the pinch effect and estimate the characteristic plasma-pinching time τ_p . *S*-shaped CVC are observed in the breakdown region at $I \parallel C_1, C_2$, but a vertical plot of $I(E)$ is usually observed at $I \parallel C_3$ (Fig. 1b). In the pre-breakdown region it is easy to estimate the electron mobility from the shape of the CVC, namely $\mu_{e0} = 7.5 \times 10^8$ cgs esu at $E \parallel C_1$ and 10^9 at $E \parallel C_3$. We took into account the decrease of the electron mobility with increasing plasma density n (electron-hole scattering⁶) and assumed that

$$\mu_e = \mu_{e0} / (1 + \alpha N),$$

where $N = n/n_0$ and $\alpha \approx 0.1$ is the electron-hole scattering parameter. The $\mu_{e0}(E)$ dependence was disregarded, since all

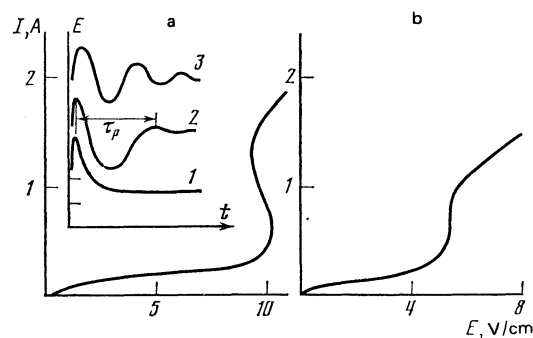


FIG. 1. Measured CVC of the alloy $\text{Bi}_{0.9}\text{Sb}_{0.1}$. a) $I \parallel C_1$, b) $I \parallel C_3$. Inset—typical scans of $E(t)$ in the given-current regime: 1—1, 2—2, 3—4 A; $\tau_p = 2 \cdot 10^{-8}$ sec at $I = 2$ A.

the CVC singularities take place in a narrow range of the field E .

We estimate now the hole mobility in the NDR region from the measured pinching time τ_p (Fig. 1a, inset), recognizing that according to Ref. 7

$$\tau_p \approx c^2 R_0^2 / 4\mu_h v_d I,$$

where $R_0 \approx 1.5 \times 10^{-2}$ cm is the transverse dimension of the sample, and v_d is the electron drift velocity ($v_d \approx 10^7$ cm/sec, see Ref. 1). It is easy to estimate that $\mu_h \approx 7.5 \times 10^7$ cgs esu. Thus, in relatively weak electric fields of the order of 10 V/cm the hole mobility in $\text{Bi}_{1-x}\text{Sb}_x$ alloys decreases radically ($\mu_e \gg \mu_h$) apparently as a result of L - T intervalley transitions of the holes when they are heated in the electric field.⁸ Assuming that the electron-hole gas temperature is 80 K (Ref. 1) we can estimate the hole diffusion coefficient at $D_h \approx 10^3$ cm²/sec. As will be shown by the calculations that follow (see Fig. 4 below), the pinch diameter calculated with this value of D_h (from the position of the maximum of H agrees well with earlier measurements⁹, viz., $r_p \approx 10^{-2}$ cm at $I = 2$ A.

Figure 2 shows the measured dependence of the impact ionization rate on E . The measurements were made using nanosecond voltage pulses, when the plasma current is low and there is no transverse breakdown. It can be seen from this figure that g is less at the orientations $\mathbf{E} \parallel C_1, C_2$ than in the case $\mathbf{E} \parallel C_3$. The possible reason is that at $\mathbf{E} \parallel C_1, C_2$ the carrier heating is slowed down by intervalley transitions, owing to the nonequivalent disposition of the valleys relative to the electric field,¹⁰ whereas all valleys are equivalent in the case $\mathbf{E} \parallel C_3$.

The $g(E)$ dependence can be approximated by the function

$$g = g_0 \exp(-E_0/E), \quad (1)$$

where at $x = 0.1$ we have for curve 1 $g_{01}(\mathbf{E} \parallel C_1) = 7.7 \times 10^9$ sec⁻¹ and $E_{01} = 39.4$ V/cm, whereas for curve 3, $g_{03}(\mathbf{E} \parallel C_3) = 1.8 \times 10^{10}$ sec⁻¹ and $E_{03} = 34$ V/cm. The error in the measurement of g did not exceed 25%.

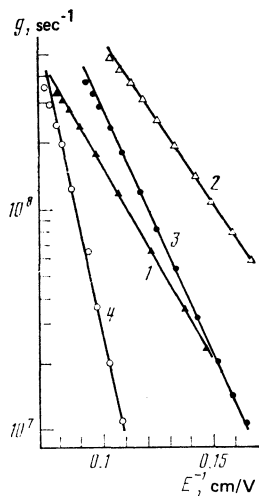


FIG. 2. Measured dependences of the rate of impact ionization on the electric field in the alloy $\text{Bi}_{1-x}\text{Sb}_x$: 1-3- $x = 0.1$, 4- $x = 0.108$; 1- $\mathbf{E} \parallel C_2$, 2- $\mathbf{E} \parallel C_3$, 3,4- $\mathbf{E} \parallel C_1$.

Taking the indicated anisotropy into account, we used in the subsequent calculations of the plasma parameters under combined-breakdown conditions an impact-ionization rate at $\mathbf{E} \parallel C_1$ in the form

$$G = g_1(E_{\text{eff}}) \cos^2 \theta + g_3(E_{\text{eff}}) \sin^2 \theta, \quad (2)$$

where $E_{\text{eff}} = E_{\text{tot}} / (1 + \beta H)$ and $E_{\text{tot}} = [E^2 + E_H^2]^{1/2}$ is the total electric field, while $\tan \theta = |E_H|/E$.

This choice of G can be justified in the following manner:

a) In the case of transverse breakdown the decisive role is played by the total electric field.^{11,12}

b) Introduction of the coefficient β (Ref. 13) reflects both the saturation of the rate of impact ionization and the increase of the threshold value of E_{tot} at which breakdown sets in,^{11,12} with increasing magnetic field. Recognizing that the criterion for the transverse breakdown in a strong magnetic field ($\mu_e H/c \gg 1$) is of the form $cE_{\text{tot}}/H > 0.2v_0$, where v_0 is the velocity of an electron having an energy equal to that of an optical phonon ($\epsilon_{\text{opt}} \approx 10$ meV, $m_e \approx 10^{-29}$ g), we easily estimate that $\beta \approx 5 \times 10^{-3}$ Oe⁻¹.

c) Introduction of the angle θ reflects the anisotropy of the transverse breakdown; in this case expression (2) is the only linear combination of g_1 and g_3 that satisfies the required limiting transitions. At $\mathbf{E} \parallel C_3$ it is necessary to make in (2) the substitution $g_{1,3} \rightarrow g_{3,1}$.

The lifetime measured at low pump levels ($n < n_0$) is, in accord with the results of Ref 4, $\tau \approx 5 \times 10^{-9}$ sec. At high pump levels ($n > 5 \times 10^{15}$ cm⁻³) bulk Auger recombination predominates. We took account in the calculations the linear and cubic bulk Auger recombinations. The coefficient of the cubic bulk recombination was assumed to be $r_3 = 10^{-23}$ sec⁻¹·cm⁻⁶.

Noticeable symptoms of impact breakdown should be observed under conditions at a nonequilibrium-plasma density $n \approx n_0$, from which follows the equality $g(E) = 1/2\tau = 10^8$ sec⁻¹. It is easy to estimate, taking (1) into account, that the steep rise of the CVC with increasing E begins at $E \approx 9$ V/cm (for $\mathbf{E} \parallel C_1$) and at $E \approx 6$ V/cm for $\mathbf{E} \parallel C_3$, in agreement with the measurement data (Fig. 1).

We proceed now to the results of calculations for a cylindrical geometry; the hole mobility was assumed isotropic ($\mu_h \ll \mu_e, \mu_h H/c \ll 1$).

The initial equations that describe the change of the density of a quasineutral plasma and of the magnetic self-field of the current can be obtained with the aid of the equations of motion of the electrons and holes, the continuity equation for the radial ambipolar field, and Maxwell's equations for the azimuthal magnetic field of the current. These are

$$\frac{\partial N}{\partial t} + \frac{1}{\rho} \frac{\partial(\rho \Gamma_p)}{\partial \rho} = G(N+1) - \frac{N}{\tau} - R_3 N^3, \quad (3)$$

$$\frac{1}{\rho} \frac{\partial(\rho H)}{\partial \rho} = \frac{4\pi}{c} e n_0 R_0 \mu_{eH} E (N+1) + \frac{4\pi e}{c^2} \mu_{eH} n_0 R_0^2 H \Gamma_p, \quad (4)$$

where

$$\Gamma_p = - \left(1 + \frac{\mu_{eH} \mu_h N H^2}{c^2 N+1} \right)^{-1} \left(\frac{D_h}{R_0^2} \frac{2N+1}{N+1} \frac{\partial N}{\partial \rho} + \frac{\mu_h \mu_{eH}}{c R_0} E H N \right)$$

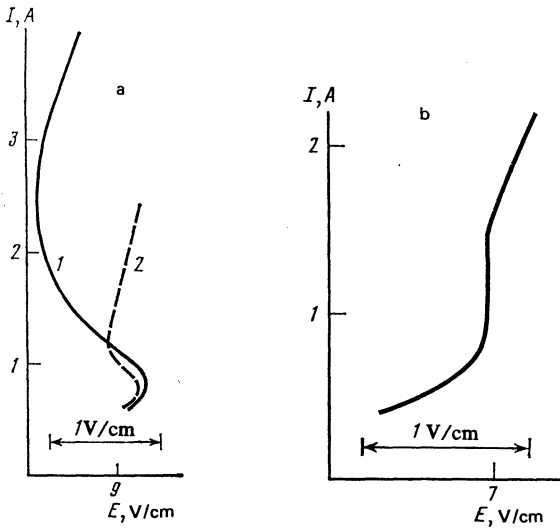


FIG. 3. Calculated CVC for the alloy $\text{Bi}_{0.9}\text{Sb}_{0.1}$: a) $\mathbf{E}\parallel C_1$, $1 - \mu_h = 7.5 \cdot 10^7$, $2 - \mu_h = 10^8$; b) $\mathbf{E}\parallel C_3$, $\mu_h = 7.5 \cdot 10^7$ (the mobility is in cgs esu units).

corresponds to the radial ambipolar flux $n_0 R_0 \Gamma_\rho$, $R_3 = r_3 n_0^2$, $\rho = r/R_0$ and $\mu_{e\parallel}$ is the electron mobility along the field \mathbf{E} .

The boundary and initial conditions are $\Gamma(\rho = 0; 1) = 0$ (a low surface-recombination rate is assumed), $H(\rho = 0) = 0$,

$$H(\rho = 1) = 2I(t)/cR_0,$$

$I(t) = I[1 - \exp(-t/\tau_p)]$ is the current, and we use in the calculations $\tau_p = 10^{-9}$ sec and $N(t = 0) = 0$.

The expression for the fields E_H that determines the value of G is

$$E_H = - \left(1 + \frac{\mu_{e\parallel} \mu_h}{c^2} \frac{NH^2}{N+1} \right)^{-1} \times \left(\frac{\mu_{e\parallel} H}{c} + \frac{D_h}{\mu_h R_0} \frac{1 - c^{-2} \mu_{e\parallel} \mu_h H^2}{N+1} \frac{\partial N}{\partial \rho} \right). \quad (5)$$

The procedure for numerically solving the problem is the following: given the distribution $N(\rho)$, we use (4) to determine E and $H(\rho)$. This is followed by solving (3) with allowance for (2) and (5) and finding the plasma-density profile at the next instant of time, and so on. The calculation is continued until a stationary state sets in. Once the steady-state values of the field E are established for a given current, it is easy to plot the static CVC, which are shown in Fig. 3. The calculated CVC agree qualitatively and quantitatively with the experimental results (Fig. 1).

The NDR segment appears at $\mathbf{E}\parallel C_1$ in the region of relatively small currents ($H_{\max} \approx 10$ Oe), when the pinch effect is weak and the linear recombination is small. In this case the plasma density is determined by the factor $G/(1/\tau - G)$, which increases abruptly when the field E_H becomes active in the ionization process. Therefore when the current (the field H) is increased the external field E that produces the given current can decrease. With further decrease of the current, the pinch effect evolves, the Auger recombination and electron-hole scattering processes become stronger, and

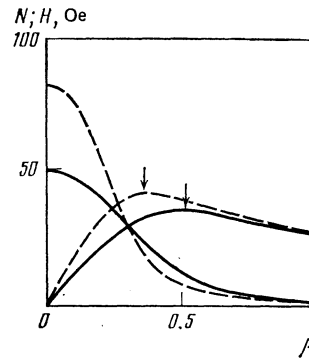


FIG. 4. Calculated profiles of the plasma density and of the magnetic field of the current at $I = 2$ A and $\mathbf{E}\parallel C_1$. The dashed and solid curves are for $\mu_h = 10^8$ and $\mu_h = 7.5 \cdot 10^7$, respectively (the mobilities are in cgs esu).

the NDR segments vanish. We note that when μ_h is increased (Fig. 3a) the S-shaped segment of the CVC is less pronounced, since the pinch effect sets in at lower currents. The vanishing of the NDR at high currents is due in part also to magnetization of the plasma.

At $\mathbf{E}\parallel C_3$, when a large coefficient of impact ionization along \mathbf{E} combines with a small one in the transverse direction, only a vertical section of the CVC is produced (Fig. 3b). It must be noted, however, that when the antimony concentration in the alloy is increased the $g(E)$ dependence becomes stronger (Fig. 2, curve 4). In this case, owing to the strong change of G with increasing E_{tot} , the CVC have segments with NDR also at $\mathbf{E}\parallel C_3$, as shown by our calculations.

Figure 4 shows typical profiles of the plasma density and of H at various hole mobilities; from these it is easy to calculate the pinch radius. The pinch effect becomes stronger with increasing μ_h . We note in this connection that in a number of our experiments the NDR segments vanish when the transverse dimension of the sample is increased by 2–3 times. With increasing R_0 , the value of E that ensures the given current decreases, and this increases the hole mobility. The latter in turn decreases E_H and enhances the plasma pinching, and it is this which leads apparently to the vanishing of the NDR segments in samples with larger dimensions.

In conclusion, we are deeply grateful to N. B. Brandt for interest in the work and for constant support.

¹We note that in the impact-ionization regime the surface generation of current,³ an effect accompanying the pinch effect, is very weakly pronounced and does not affect the shape of the CVC.

¹N. B. Brandt, E. A. Svistov, E. A. Svistova, and G. D. Yakovlev, Zh. Eksp. Teor. Fiz. **61**, 1078 (1971) [Sov. Phys. JETP **34**, 575 (1972)].

²M. Toda and M. Glicksman, Phys. Rev. A, **140**, 1317 (1965).

³W. Schillinger, IBM J. Res. Dev. **8**, 295 (1964).

⁴N. B. Brandt, E. V. Bogdanov, V. M. Manankov, and G. D. Yakovlev, Fiz. Tekh. Poluprov. **15**, 810,813 (1981) [Sov. Phys. Semicond. **15**, 464,465 (1981)].

⁵B. Ancker-Johnson, R. W. Cohen, and M. Glicksman, Phys. Rev. **124**, 1745 (1961).

⁶E. Conwell and V. F. Weisskopf, Phys. Rev. **77**, 388 (1950).

⁷V. V. Vladimirov, Usp. Fiz. Nauk **117**, 79 (1975) [Sov. Phys. Usp. **18**, 690 (1975)].

- ⁸J. S. Lannin and K. F. Cuff, *The Physics of Semimetals and Narrowgap Semicond.*, Proc. Int. Conf. Dallas, TX, Pergamon, 1971, p. 85.
- ⁹N. B. Brandt, B. A. Akimov, *et al.*, Abstracts, 3rd Symp. on Semimetals and Narrow-Gap Semiconductors, L'vov, 19792, p. 49.
- ¹⁰G. A. Mironova, M. V. Sudakova, and Ya. G. Pomarev, *Zh. Eksp. Teor. Fiz.* **78**, 1830 (1980) [*Sov. Phys. JETP* **51**, 918 (1980)].
- ¹¹H. Reuter and K. Hübner, *Phys. Rev.* **B4**, 2575 (1971).
- ¹²A. A. Andronov, V. A. Valov, V. A. Kozlov, and L. S. Mazov, Preprint, Appl. Phys. Inst. USSR Acad. Sci. No. 2, Gor'kiï, 1980.
- ¹³V. V. Vladimirov, V. N. Gorshkov, A. G. Kollyukh, and V. K. Malyutenko, *Zh. Eksp. Teor. Fiz.* **82**, 2001 (1982) [*Sov. Phys. JETP* **55**, 1150 (1982)].

Translated by J. G. Adashko